agriculture

Article

Comparing Simulated Jujube Evapotranspiration from P–T, Dual Kc, and S–W Models against Measurements Using a Large Weighing Lysimeter under Drip Irrigation in an Arid Area

Pengrui Ai *, Yingjie Ma and Ying Hai

College of Hydraulic and Civil Engineering, Xinjiang Agricultural University, Urumqi 830052, China
* Correspondence: xjaipengrui@xjau.edu.cn; Tel.: +86-15276632503

Abstract: Accurate prediction of orchard evapotranspiration (ET) can optimize orchard water management. Based on the jujube (*Zizyphus jujuba*), ET was continuously measured from 2016 to 2019 using a large weighing lysimeter; the actual jujube ET was compared with the ET simulated with the Priestley–Taylor (P–T), Dual Crop Coefficient (Dual Kc), and Shuttleworth–Wallace (S–W) models, to verify the accuracy of the three models. The results showed that, from 2016 to 2019, the whole growth period of jujube ET was 532–592 mm and the crop coefficient was 0.85–0.93. The basal crop coefficients of the calibrated Dual Kc model were 0.4, 1.0, and 0.5 at the initial, middle, and ending growth stages, respectively. The overall simulation error of the Dual Kc model was low, and simulations were stable during the four years of the study. However, because of rough estimation the water stress coefficient (K_s) simulation accuracy will be reduced in the case of serious water shortage. The simulation error of the S–W model was greater than the simulation error of the Dual K_c model, and the simulations were unstable and vulnerable to interannual changes. The simulation error of the traditional P–T model was large. When the parameter "α" solution method was improved, the simulation accuracy was significantly improved, and the P–T model's simulation accuracy was only slightly lower than that of the Dual Kc model. However, the model was easily affected by changes in net radiation and air temperature. Therefore, the Dual Kc model is recommended for estimating the ET of young jujube trees in arid areas.

Keywords: jujube; large weighing lysimeter; Priestley–Taylor model; dual crop coefficient model; Shuttleworth–Wallace model

check for updates

Citation: Ai, P.; Ma, Y.; Hai, Y. Comparing Simulated Jujube Evapotranspiration from P–T, Dual Kc, and S–W Models against Measurements Using a Large Weighing Lysimeter under Drip Irrigation in an Arid Area. *Agriculture* **2023**, *13*, 437. https://doi.org/10.3390/agriculture13020437

Academic Editor: Aliasghar Montazar

Received: 31 December 2022
Revised: 7 February 2023
Accepted: 10 February 2023
Published: 13 February 2023

1. Introduction

Jujube (*Zizyphus jujuba*) is the most important horticultural crop in Xinjiang, China. This area is the major jujube producer in the world, covering 476,250 ha and producing a crop of 3,470,114 tons [1]. The quality of the fruit coming from this area is highly appreciated in the domestic and international markets. These facts reveal the economic importance of this crop for the region, and its production is the main source of rural employment and economic income in the area. However, Xinjiang is located in the hinterland of Eurasia. The abundant light and heat resources not only improve the quality of jujube fruit, but also increase surface evapotranspiration intensity that can result in a serious shortage of water resources. In order to ensure the yield and quality of crops in this area, local farmers have continuously increased the amount of water applied to crops. Agricultural water consumption accounts for 89.45% of the total water supply in Xinjiang, putting severe pressure on the normal water demands of various other industries [1]. This situation has led to a conflict of interests between agriculture and other industries, and demands management solutions for sustainable jujube production in this environmentally sensitive area.

In this sense, jujube production must employ proper irrigation management that is based on accurate assessment of jujube water requirement in this area. The dual crop coefficient (Dual Kc) model is one of the most frequently used models employed to evaluate and predict crop water demand [2]. This model clearly describes the evapotranspiration (ET) process and its influencing factors by considering aerodynamic and vegetation characteristics, and determines the crop coefficient [3]. However, crop coefficient is highly dependent on the cultivar, local climatic conditions, and crop management, among other factors [4]. Therefore, the Food and Agriculture Organization has determined basal crop coefficients for the main crops cultivated by human beings according to the climatic conditions of semi-humid areas [5], and these have been used to improve the applicability of the Dual Kc model around the world. However, Tian et al. [6] reported that arid climates significantly increase the ET and K_{cb} of cotton (*Gossypium hirsutum* L.), especially under extremely high temperature conditions. Under arid climate conditions, the basal crop coefficients (K_{cb}) of cotton for the initial, mid-season, and end-season periods were 0.20, 0.90, and 0.50, respectively, while Peddinti et al. [7] reported that the three-stage basal crop coefficients were 0.43, 0.78, and 0.80, respectively, for citrus orchards. These K_{cb} values varied significantly from FAO-established K_{cb} values. Thus, K_c values may differ substantially due to differences in ground cover (f_c), plant height (h), planting density, and plant age, as has been previously discussed by Rallo et al. [8] and Lozano et al. [9]. The parameters must be corrected when using the Dual Kc model to estimate evapotranspiration of drip-irrigated jujube in arid oasis areas.

The Priestley–Taylor (P–T) model is based on the assumption that the influence of atmospheric aerodynamics on ET are less than the influence of radiation [10]. It is calculated based on average temperature and net radiation. Because the model requires fewer meteorological variables as inputs, it is widely used in forest, grassland, and agronomic studies, especially in areas with high net radiation intensity [11–13]. Additionally, in order to correct for the influence of advection on transpiration, the model uses an empirical coefficient "α" for correction. Previous research has shown that there are many factors that may affect "α": it has been shown to be equal to 1.26 where there is a wet underlying surface [14]; equal to 0.7~1.6 for landscape ecosystems [15]; and equal to 1.5~2.0 for arid climates [16]. Therefore, the value of "α" is often different for factors such as lower mean annual temperature and other climate characteristics.

The Shuttleworth–Wallace (S–W) model is a dual source model for estimating ET components. Its theoretical basis is the Penman–Monteith equation, which has two parts: the soil surface and the plant surface [17]. For the processes of soil evaporation and canopy ET, the model primarily regulates energy transfer intensity through canopy resistance and soil surface resistance (r_s^c and r_s^s). Additionally, in order to account for the impact of external environmental factors on crop ET, three aerodynamic resistances (r_a^a, r_a^c, r_a^s) are used to regulate transport intensity in the atmosphere, canopy, and soil, respectively. Previous studies indicated that the S–W model performed well in estimating the ET of rice (*Oryza sativa* L.) [18], cucumbers (*Cucumis sativus* L.) [19], grapes (*Vitus vinifera* L.) [20], apples (*Malus sylvestris* (L.) Mill var. domestica (Borkh.) Mansf.) [21], and other plant species. The simulation accuracy of S–W is higher than other models, especially under conditions of partial coverage [22]. However, studies are still lacking regarding whether S–W can produce ideal simulation accuracy for young jujube trees grown in an arid environment.

In order to determine the optimum model for estimating jujube ET grown under drip irrigation in an arid area, we conducted a four-year irrigation experiment in a jujube garden equipped with a large weighing lysimeter. Based on meteorological variables and plant physiological and morphological observations, water consumption during the entire jujube growing season was simulated. The objective of this research was based on measuring the jujube ET using a large weighing lysimeter to evaluate the applicability and parameter sensitivity of three ET models (Dual Kc, P–T, and S–W), in order to provide evidence to assist farmland managers in choosing the optimum ET model for agricultural water management.

2. Materials and Methods

2.1. Study Location

The study was conducted at the Experimental Station of Xinjiang Agricultural University, located in the Aksu region of Xinjiang (41°16′ N, 80°14′ E; altitude, 1133 m, Figure 1) from 2015 to 2019. The climate at this location is a typical temperate arid climate (Koppen: Bwk). Average annual values (2008–2019) of climate variables were: precipitation (74 mm), temperature (11.4 °C), total sunshine hours (2728–3014 h), and frost-free period (203–224 day). The soil of the experimental field was predominantly a sandy loam, with field capacity of 28% (volumetric water content) and wilting point of 8% (volumetric water content). Jujube at this location buds around Late April and is harvested at the end of October. Jujube roots are mainly distributed in the 0–100 cm soil layer [23].

Figure 1. Location of the study area.

2.2. Experimental Design

The crops used in this study were 5-year-old jujube (*Zizyphus jujuba*), planted in rows with a spacing of 4 m × 1 m. The drip tape lines were located on either side of the tree row, 40 cm away from the tree row. The dripper discharge rate was 1.38 L/h. The P–M model [5] was used to guide irrigation in the experimental field, and irrigations were applied every seven days (Table 1). The irrigation amount was determined as the calculated cumulative $ET = ET_0 \times K_c$ since the previous irrigation. Jujube crop coefficients (K_c) were calculated as described by Hong et al. [24]. Additionally, in order to increase the sugar content in the fruit, irrigation was stopped in the later stage of fruit enlargement.

Table 1. Irrigation design for jujube in a large weighing lysimeter from 2016 to 2019 in the Aksu region, Xinjiang, China.

Growing Season	Spring Irrigation	Budding	Flower and Fruit Setting	Fruit Enlargement	Fruit Mature	Entire Season
2016	40 mm	78 mm	158 mm	205 mm	35 mm	516 mm
2017	40 mm	95 mm	159 mm	201 mm	35 mm	530 mm
2018	40 mm	108 mm	157 mm	199 mm	35 mm	539 mm
2019	40 mm	102 mm	143 mm	199 mm	35 mm	519 mm

Three large weighing lysimeters were randomly arranged in a 3000 m^2 jujube field. A large weighing lysimeter (BSI-GDZSY2.2*3*2.5, Xi'an BiShui Environmental New Technology Co., Ltd., Xi'an, China) was used in the experiment to determine ET (Figure 2). The electronic weighing system comprised the soil system, weighing system, water supply, drainage system, and data acquisition system. The surface area of the lysimeter was 6.6 m^2, the soil depth was 2.5 m (0.3 m inverted filter, 2.2 m soil layer). The weighing system adopts a lever-type structure, the system resolution was 5 g, the measurement accuracy was $\pm$50 g, and the range was 0~6500 kg. The accuracy of the water leakage measuring system was $\pm$2.5%. The system was equipped with power-off protection measures, which can work for more than 48 h after power-off. The change of soil weight was recorded every 30 min (change of soil weight = jujube evapotranspiration).

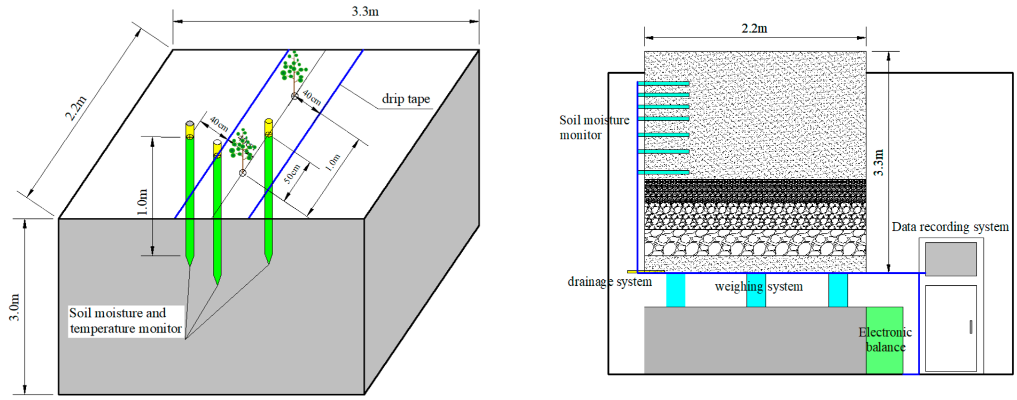

Figure 2. The large weighing lysimeter setup in the Aksu region, Xinjiang, China.

2.3. Measurements

(1) Temperature, radiation, and rainfall were measured every 30 min using a Watchdog small automatic weather station (Model 2700, Spectrum Technologies, Inc, Aurora, IL, USA).
(2) The soil moisture content in the 0–100 cm layer was measured with a soil moisture and temperature monitor (ET-100, Insentek Co., Ltd., Hangzhou, China), and the data were recorded every 30 min. The instrument layout position was at 40 cm (between jujube plants) and 40 cm from the jujube row.
(3) The leaf area index (LAI) of jujube plants in the Large Weighing Lysimeter was observed every 10–20 days using a HemiView plant canopy analyzer (HMV1 v9, Delta-T Devices, Cambridge, UK).
(4) The plant height of jujube plants was measured 1–2 times with a ruler in each growing season. Plant height (h) ranged from 1.21 to 2.79 m during the 2016 to 2019 study period.
(5) Soil evaporation was determined using micro-lysimeters [25]. Each micro-lysimeter was 11 cm in diameter and 15 cm in depth. Measurements were made daily at 10:00 A.M. to determine water loss. The jujube micro-lysimeters were placed at 50 cm (between jujube plants) and 40 cm from the jujube row.

2.4. Shuttleworth–Wallace Model

The S–W model is the P–M model expanded into two parts: canopy and soil. According to Beer's Law, solar radiation is distributed between the canopy and the soil surface, and the ET of the entire underlying surface is calculated using the following formulas [17]:

$$\lambda ET = C_c PM_c + C_s PM_s \tag{1}$$

$$PM_c = \frac{\Delta A + (\rho C_P VPD - \Delta r_a^c A_s)/(r_a^a + r_a^c)}{\Delta + \gamma(1 + r_s^c/(r_a^a + r_a^c))} \tag{2}$$

$$PM_s = \frac{\Delta A + (\rho C_P VPD - \Delta r_a^s (A - A_s))/(r_a^a + r_a^s)}{\Delta + \gamma(1 + r_s^s/(r_a^a + r_a^s))} \tag{3}$$

$$A = R_n - G \tag{4}$$

$$A_s = R_{ns} - G \tag{5}$$

$$C_c = (1 + R_c R_a / R_s (R_c + R_a))^{-1} \tag{6}$$

$$C_s = (1 + R_s R_a / R_c (R_s + R_a))^{-1} \tag{7}$$

$$R_a = (\Delta + \gamma) r_a^a \tag{8}$$

$$R_s = (\Delta + \gamma) r_a^s + \gamma r_s^s \tag{9}$$

$$R_c = (\Delta + \gamma) r_a^c + \gamma r_s^c \tag{10}$$

$$R_{ns} = R_n \times e^{-C \times LAI} \tag{11}$$

Δ, VPD, P, ρ are related to meteorological factors, and are calculated as given in Allen et al. [5]:

$$\Delta = \frac{4098[0.6108 \exp(\frac{17.27T_a}{T_a + 237.3})]}{(T_a + 237.3)^2} \tag{12}$$

$$VPD = 0.6108 \exp(\frac{17.27T_a}{T_a + 237.3}) \times (1 - RH) \tag{13}$$

$$\gamma = 0.665 \times 10^{-3} \times P \tag{14}$$

$$P = 101.3[(293 - 0.0065 \times H)/293]^{5.26} \tag{15}$$

$$\rho = 1.293 \times (P/101.325) \times \left(\frac{273.15}{273.15 + T_a}\right) \tag{16}$$

Boundary layer resistance r_a^c was calculated as given in Zhou et al. [26]:

$$r_a^c = r_b \sigma_b / LAI \tag{17}$$

$$r_b = \frac{100}{n} \frac{(w/u_h)}{1 - \exp(-n/2)} \tag{18}$$

$$n = \begin{cases} 2.5 & 1 \le h \\ 2.036 + 0.194h & 1 < h < 10 \\ 4.25 & h \ge 10 \end{cases} \tag{19}$$

Canopy resistance r_s^c was calculated as given in Chen and Dudhia [27], Gardiol et al. [28], and Tourula and Heikinheimo [29]:

$$r_s^c = \frac{r_{s\ min}}{LAI_{eff} \times F_1(S) \times F_2(VPD) \times F_3(T) \times F_4(\theta)} \tag{20}$$

$$LAI_{eff} = \begin{cases} LAI & LAI \le 2 \\ 2 & 2 < LAI < 4 \\ LAI/2 & LAI \ge 4 \end{cases} \tag{21}$$

$$F_1(S) = \frac{\left(\frac{r_{s\ min}}{r_{s\ max}}\right) + S}{1 + S} \tag{22}$$

$$S = 0.55 \frac{R_n}{LAI} \tag{23}$$

$$F_2(VPD) = 1 - g \times VPD \tag{24}$$

$$F_3(T) = 1 - 0.0016(25 - T)^2 \tag{25}$$

$$F_4(\theta) = \begin{cases} 1 & \theta > \theta_t \\ \frac{\theta - \theta_w}{\theta_t - \theta_w} & \theta_w \leq \theta \leq \theta_t \\ 0 & \theta < \theta_w \end{cases} \tag{26}$$

Soil surface resistance r_s^s was calculated as given in Villagarcía et al. [30]:

$$r_s^s = 250\left(\frac{\theta_t}{\theta}\right) - 100 \tag{27}$$

Aerodynamic resistance between vegetation canopy height and reference height r_a^a, and aerodynamic resistance between the soil surface and vegetation canopy r_a^s were calculated as given in Shuttleworth and Wallace [17]:

$$r_a^a = 0.25LAI\ r_a^a(a) + 0.25(4 - LAI)r_a^a(0) \tag{28}$$

$$r_a^s = 0.25LAI\ r_a^s(a) + 0.25(4 - LAI)r_a^s(0) \tag{29}$$

$$r_a^a(0) = \frac{ln\frac{x}{z_0'}\ ln\frac{x}{z_0'}}{k^2u} - r_a^s(0) \tag{30}$$

$$r_a^s(0) = \frac{ln\frac{x}{z_0'}\ ln\frac{d+z_0}{z_0'}}{k^2u} \tag{31}$$

$$r_a^a(a) = \frac{\ln\frac{x-d}{z_0}}{k^2u}[\ln\frac{x-d}{h-d} + \frac{h}{n(h-d)}\left[\exp\left(n\left(1 - \frac{d+z_0}{h}\right)\right) - 1\right]] \tag{32}$$

$$r_a^s(a) = \frac{\ln\frac{x-d}{z_0}}{k^2u}\frac{h}{n(h-d)}[\exp n - \exp\left(n\left(1 - \frac{d+z_0}{h}\right)\right)] \tag{33}$$

$$z_0 = \begin{cases} z_0' + 0.3hX^{0.5} & 0 < X < 0.2 \\ 0.3h\left(1 - \frac{d}{h}\right) & 0.2 \leq X < 1.5 \end{cases} \tag{34}$$

$$d = 1.1h\ \ln\left(1 + X^{0.25}\right) \tag{35}$$

$$X = c_d \times LAI \tag{36}$$

where:

r_a^a is the aerodynamic resistance between vegetation canopy height and reference height, s m^{-1};
r_a^s is the aerodynamic resistance between the soil surface and the vegetation canopy, s m^{-1};
r_a^c is the boundary layer resistance, s m^{-1};
r_s^c is the canopy resistance, s m^{-1};
r_s^s is the soil surface resistance, s m^{-1}.

The meanings of other symbols are shown in Table 2.

Table 2. List of symbols used in S–W, Dual Kc, P–T models.

Symbol	Name	Unit
ρ	Density of dry air	kg m^{-3}
γ	Psychrometric constant	Pa °C^{-1}
Δ	Slope of saturation to vapor pressure curve	Pa °C^{-1}
VPD	Water vapor pressure deficit	kPa
R_n	Net radiation flux	MJ m^{-2} day^{-1}
G	Surface soil heat flux	MJ m^{-2} day^{-1}
LAI	Leaf area index	m^2 m^{-2}
T_a	Air temperature	°C
RH	Air relative humidity	%

Table 2. *Cont.*

Symbol	Name	Unit
P	Atmospheric pressure	kPa
H	Altitude	m
r_b	Mean boundary layer resistance	s m^{-1}
w	Canopy characteristic leaf width	m
u_h	Wind speed at the top of canopy	m s^{-1}
h	Mean height of the crop	m
n	Eddy diffusion decay constant	-
$r_{s\ min}$	Minimum canopy resistance	-
LAI_{eff}	Effective leaf area index	-
θ_w	Wilting coefficient of soil	%
θ_t	Soil water-holding capacity	%
θ	Soil moisture of the soil root system	%
x	Reference height	m
z_0	Roughness length	m
d	Zero-plane displacement	m
u	Wind speed	m s^{-1}
ET_0	Reference evapotranspiration	mm day^{-1}
ET	Crop evapotranspiration	mm day^{-1}
λ	Latent heat flux	2.45 MJ kg^{-1} [5]
C_P	Specific heat capacity of air	0.001013 J kg^{-1} °C^{-1} [5]
C	Extinction coefficient of light	0.7 [16]
σ_b	Shielding factor	0.5 [16]
$r_{s\ max}$	Maximum stomatal resistance value	5000 m s^{-1} [31]
g	Empirical coefficient	0.25 kPa^{-1} [32]
z'_0	Effective roughness length	0.02 m [33]
k	von Kármán constant	0.41 [21]
c_d	Mean drag coefficient for leaves	0.07 [26]

2.5. Dual Crop Coefficient Model

The dual crop coefficient (Dual Kc) model was given by Allen et al. [4] as:

$$ET = (K_s \cdot K_{cb} + K_e)ET_0 \tag{37}$$

where: ET is the evapotranspiration, mm·d^{-1};
K_s is the water stress coefficient;
K_{cb} is the basal crop coefficient;
K_e is the soil evaporation coefficient.

For determination of the related parameters in the Dual Kc model, refer to Allen et al. [5]. There is no reference value for the basal crop coefficient for jujube in FAO-56. In this study, the initial value of the basal crop coefficient was determined by reference to other fruit trees (stone fruit). In addition, jujube is a drought-tolerant crop. It has waxy layers on its leaves, which can reduce transpiration. The ability of its leaves to prevent water loss is significantly greater than that of other crops. The basal crop coefficient and the soil water consumption coefficient will therefore be reduced.

The soil parameters and crop parameters of the model were calibrated by trial-and-error using crop ET data measured with a large weighing lysimeter in 2016 [34]. First, soil parameters were held constant, and the crop parameters adjusted to reduce simulation errors. The crop parameters were then kept unchanged while the soil parameters were adjusted based on measured soil evaporation, until the simulation error was minimal and stable. The calibrated parameters are shown in Figure 3 and Table 3.

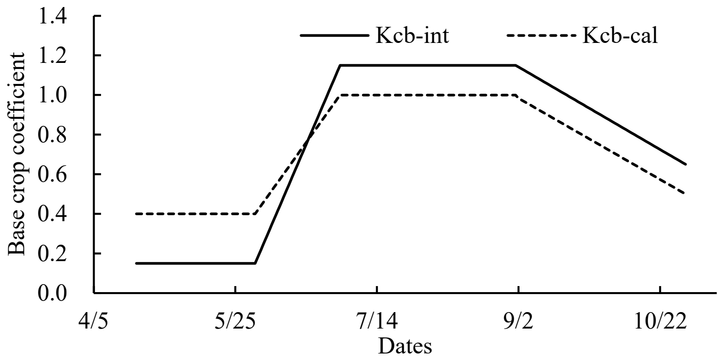

Figure 3. Basal crop coefficient initial values ($K_{cb\text{-}int}$) and calibrated values ($K_{cb\text{-}cal}$).

Table 3. Initial and calibrated values of soil parameters and crop-related parameters in the dual crop coefficient model.

Relevant Parameters		Initial Values	Calibrated Values
Soil parameters	Z_e (m)	0.10	0.15
	TEW (mm)	26.00	39.00
	REW (mm)	11.00	9.00
Crop parameters	$K_{cb\text{-}int}$	0.45	0.40
	$K_{cb\text{-}mid}$	1.10	1.00
	$K_{cb\text{-}end}$	0.85	0.50
	ρ	0.65	0.40

Note: Z_e, depth of surface soil layer subjected to drying by evaporation; TEW, total evaporable water; REW, readily evaporable water; $K_{cb\text{-}int}$, crop coefficient during the initial growth stage; $K_{cb\text{-}mid}$, crop coefficient during the mid-season growth stage; $K_{cb\text{-}end}$, crop coefficient at end of the late season growth stage; ρ, evapotranspiration depletion factor.

2.6. Priestley–Taylor Model

The Priestley–Taylor (P–T) model was formulated as given in Priestley and Taylor [10]:

$$ET = \alpha \frac{\Delta}{\Delta + \gamma} \frac{R_n - G}{\lambda} \tag{38}$$

where: α is an empirical coefficient.

In this study, the value of "α" was calculated based on the crop ET value measured using a large weighing lysimeter in 2016. The determination of "α" was resolved in three ways: (1) P–T_a: linear fitting in each of four different growth periods; (2) P–T_b: the mean value of "α" throughout the whole growth period; (3) P–T_c: a quadratic function fitting over the entire growth period. The results are shown in Figure 4 and Table 4.

2.7. Parameters for Sensitivity Analysis

T_a, RH, R_n, LAI, h_c, and θ were selected for relative sensitivity analysis because they have important influences on crop evapotranspiration [35]. Only one parameter was varied while the remaining parameters remained unchanged for the simulations conducted at each of nine disturbance steps (the disturbance amounts were −20%, −15%, −10%, −5%, 0, 5%, 10%, 15%, and 20%). The relevant calculation formula for sensitivity was [36]:

$$S = \frac{\sum_{i=1}^{n-1} \frac{(M_{i+1} - M_i)/M_a}{(P_{i+1} - P_i)/P_a}}{n-1} \tag{39}$$

where:

S is the sensitivity coefficient;
M_{i+1} and M_i are the ET simulation values of the $i+1$ and i parameters, respectively;
M_a is the mean value of the two simulated ET values;

P_{i+1} and P_i are the input values of the $i+1$ and i parameters, respectively; P_a is the mean value of the two input parameters.

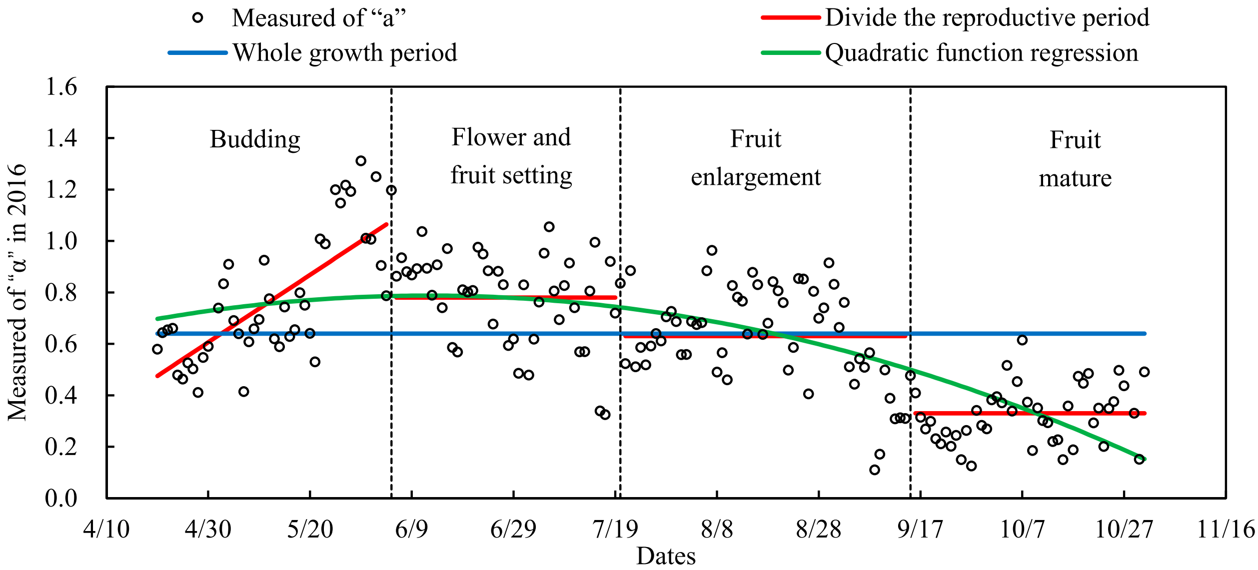

Figure 4. Fitted curve for parameter "α" in 2016.

Table 4. Calculation formulas for parameter "α" in 2016.

Different Fitting Methods	Budding	Flower and Fruit Setting	Fruit Enlargement	Fruit Mature
P−T_a(improved)	α= 1.3108 x−0.9661	α = 0.78	α = 0.63	α = 0.33
P–T_b(improved)		$\alpha = -0.3204\ x^2 + 1.0457\ x - 0.0657$		
P–T_c(original)		α = 0.64		

Note: x = day of year ×0.01; P–T_a, divide the reproductive period; P–T_b, quadratic function regression; P–T_c, whole growth period.

According to the S value, the relative sensitivity of ET to input parameters was divided into five levels [36] (Table 5).

Table 5. Sensitivity level classifications.

Levels	"S" Value Range	Relative Sensitivity
I	$\lvert S\rvert < 0.10$	Insensitive
II	$0.10 \le \lvert S\rvert < 0.25$	Minor sensitivity
III	$0.25 \le \lvert S\rvert < 0.50$	Sensitive
IV	$0.50 \le \lvert S\rvert < 1.00$	More sensitive
V	$\lvert S\rvert \ge 1.00$	Very sensitive

2.8. Evaluation of Model Performance

The following statistical indices were calculated for validating the accuracy of the S–W, Dual Kc, and P–T models [37]:

$$RMSE = \sqrt{\frac{\sum_{i=1}^{n}(O_i - P_i)^2}{n}} \tag{40}$$

$$MAE = \frac{1}{n}\sum_{i=1}^{n}|O_i - P_i| \tag{41}$$

$$RSR = \frac{\left[\sum_{i=1}^{n}(O_i - P_i)^2\right]^{0.5}}{\left[\sum_{i=1}^{n}\left(O_i - \overline{P}\right)^2\right]^{0.5}} \tag{42}$$

$$NSE = 1 - \frac{\sum_{i=1}^{n}(O_i - P_i)^2}{\sum_{i=1}^{n}(O_i - \overline{O})^2} \quad (43)$$

$$d_{IA} = 1 - \frac{\sum_{i=1}^{n}(O_i - P_i)^2}{\sum_{i=1}^{n}\left(\left|O_i - \overline{O}\right| + \left|P_i - \overline{O}\right|\right)^2} \quad (44)$$

$$PBIAS = 100\frac{\sum_{i=1}^{n}(O_i - P_i)}{\sum_{i=1}^{n} O_i} \quad (45)$$

where:

$RMSE$ is the root mean square error;
MAE is the mean absolute error;
RSR is the ratio of RMSE to the standard deviation of observed data;
NSE is the Nash–Sutcliffe efficiency coefficient;
d_{IA} is the index of agreement;
$PBIAS$ is the percent bias, the average tendency of predicted values to be larger or smaller than observed values;
n is the number of observations;
O_i and P_i are the observed and estimated values, respectively;
$\overline{O}$ and $\overline{P}$ are the average observed and average estimated values, respectively.

In this study, NSE and RSR were both used to evaluate the models (Table 6) [38]. For special cases, we graded the model performance based on the lower of the two evaluation parameters. For example, if the NSE of a model was graded as "excellent", and the RSR was graded as "Good", then the overall evaluation of the model was graded as "Good".

Table 6. Model grade evaluation.

Grade	NSE	RSR
Excellent	(0.75–1.00)	(0.0–0.5)
Good	(0.65–0.75)	(0.5–0.6)
Adequate	(0.50–0.65)	(0.6–0.7)
Unacceptable	(0.00–0.50)	(0.7–1.0)

3. Results

3.1. Environmental Parameters, Plant Height, LAI, and ET

During the 2016–2019 growing seasons, LAI and plant height (h_c) varied in a similar pattern. LAI sharply increased until late July, when maximum values occurred (1.40–1.80 m^2 m^{-2}) and then slowly decreased until the end of the growing season (Figure 5). The general trend of h_c was similar to that of LAI, and the peak also appeared in late July (Figure 5). Ranges of daily mean values of ET, ET_0, K_c, and rainfall in 2016–2019 were 532–592 mm, 625–673 mm, 0.85–0.93, and 57.3–98.8 mm, respectively (Figure 6 and Table 7). There were a few leaves in the canopy at budding, and the crop coefficient was 0.82–0.89. Then, with the development of the canopy, the crop coefficient reached maximum values of 0.86–1.03 in the flower, fruit setting, and fruit enlargement stages. When the jujube fruit matured, the irrigation amount decreased significantly, and the crop coefficient was only 0.56–0.77. By the end of the growing season, the crop coefficient was 0.85–0.93. Therefore, the ET of jujube was mainly affected by ET_0 (meteorological factors) during the 2016 to 2019 study period, and K_c over the entire season increased with increasing tree age.

(1) Linear relationship between "y = LAI of jujube" and "x = Day of year":

2016: $y = -0.81\times10^{-6} x^2 + 3.95\times10^{-2} x - 3.42$ $R^2 = 0.9796$
2017: $y = -0.83\times10^{-6} x^2 + 4.10\times10^{-2} x - 3.50$ $R^2 = 0.9727$
2018: $y = -0.91\times10^{-6} x^2 + 4.47\times10^{-2} x - 3.81$ $R^2 = 0.9743$
2019: $y = -0.97\times10^{-6} x^2 + 4.81\times10^{-2} x - 4.15$ $R^2 = 0.9817$

(2) Linear relationship between "y = Plant height of jujube" and "x = Day of year":

2016: $y = -0.0027\ x^2 + 1.1196\ x + 29.417\ R^2 = 0.9154$

2017: $y = -0.0036\ x^2 + 1.6155\ x - 3.1431\ R^2 = 0.8925$

2018: $y = -0.0040\ x^2 + 1.8749\ x - 0.8212\ R^2 = 0.9466$

2019: $y = -0.0031\ x^2 + 1.3996\ x + 87.520\ R^2 = 0.9676$

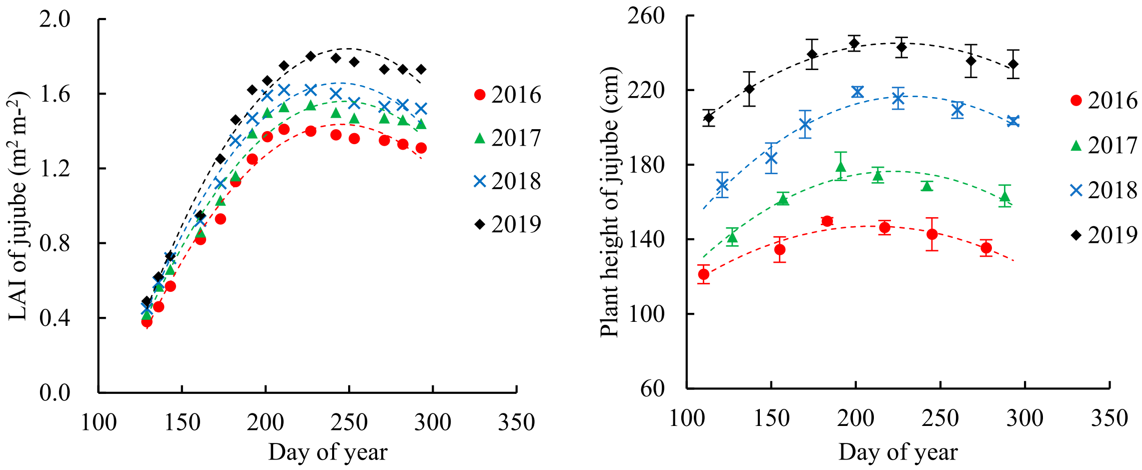

Figure 5. Seasonal variations of LAI and plant height during the 2016–2019 study period in the Aksu region, Xinjiang, China.

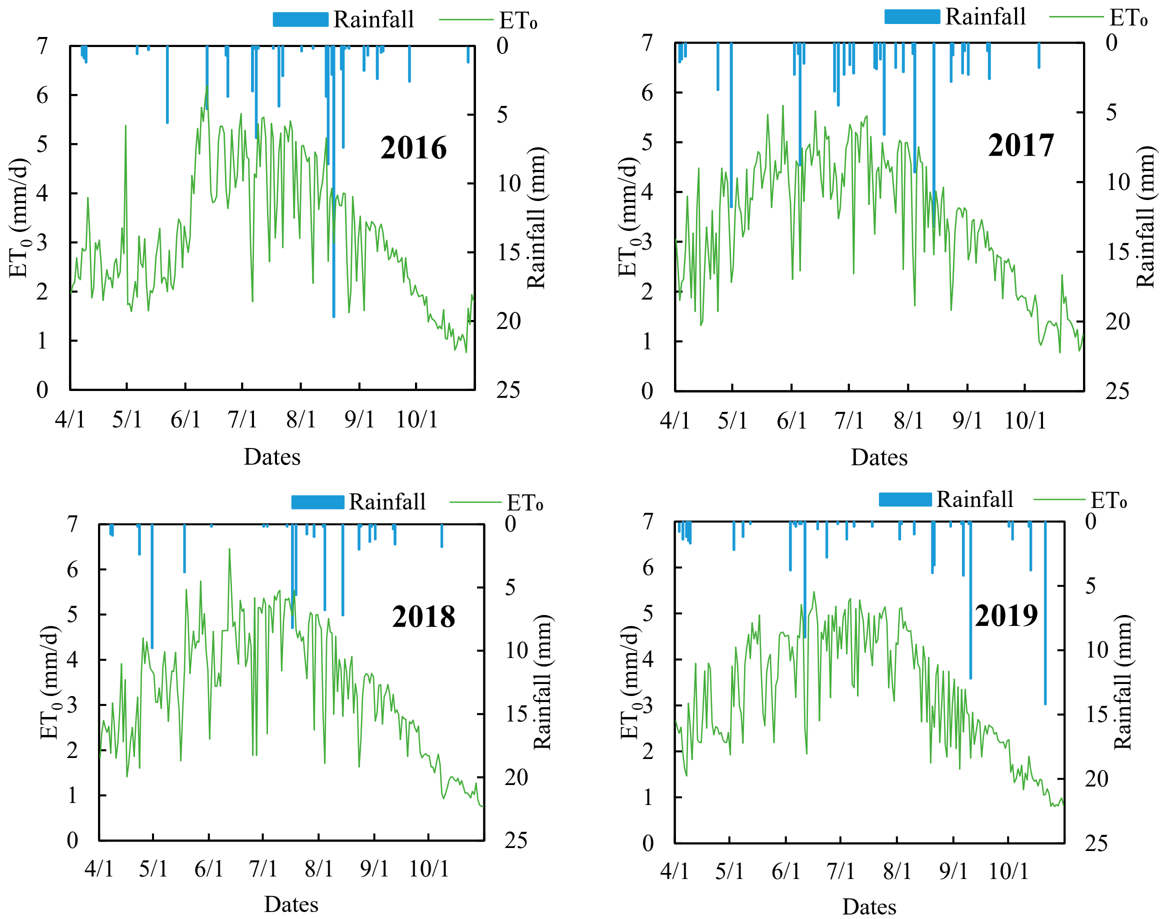

Figure 6. Rainfall and ET_0 from 2016 to 2019 in the Aksu region, Xinjiang, China.

Table 7. Jujube evapotranspiration (ET) measured using a large weighing lysimeter during several growth stages during the 2016–2019 study period in the Aksu region, Xinjiang, China, and the corresponding calculated reference evapotranspiration (ET_0) and crop coefficients (K_c).

Year	2016			2017		
	ET (mm)	ET_0 (mm)	K_c	ET (mm)	ET_0 (mm)	K_c
Budding	100.62	122.85	0.82	155.44	184.62	0.84
Flower and fruit setting	202.85	208.48	0.97	195.77	206.61	0.95
Fruit enlargement	183.86	213.29	0.86	207.61	203.78	1.02
Fruit mature	44.72	80.25	0.56	53.86	77.55	0.69
Entire season	532.05	624.86	0.85	612.68	672.56	0.91
Year	**2018**			**2019**		
	ET (mm)	ET_0 (mm)	K_c	ET (mm)	ET_0 (mm)	K_c
Budding	151.85	174.20	0.87	146.58	165.02	0.89
Flower and fruit setting	198.40	211.35	0.94	205.38	199.73	1.03
Fruit enlargement	192.84	204.17	0.94	193.18	199.99	0.96
Fruit mature	53.00	73.46	0.72	46.74	74.67	0.63
Entire season	596.08	663.18	0.90	591.88	639.41	0.93

3.2. Comparisons of Daily Jujube ET Estimated with the P–T Model and Measured Using a Large Weighing Lysimeter

Comparisons between daily ET estimated with the P–T_a, P–T_b, and P–T_c models and measurement using a large weighing lysimeter (ET_{mea}) from 2016 to 2019 are presented in Table 8. In comparison with P–T_a and P–T_b, the RMSE with P–T_c was larger (about 14% greater during the four years). The linear regression slopes ("b") ranged from 0.59 to 0.69, indicating that the model produced large errors. When the measured values were low, the model noticeably overestimated crop ET. In addition, the R^2 values for ET_{P-Tc} vs. ET_{mea} ranged from 0.62 to 0.74, indicating that the simulated and measured values were statistically similar. However, the values were still significantly lower than those observed for P–T_a and P–T_b. The simulation results for P–T_c during the four years were graded by NSE and RSR as "Adequate" or "Unacceptable", respectively. Thus, this model was unacceptable.

Table 8. Error analysis for daily jujube evapotranspiration (ET) estimated with the P–Ta, P–Tb, and P–T models compared with ET measured using a large weighing lysimeter during the 2016–2019 study period in the Aksu region, Xinjiang, China.

Year	Model	b	R^2	RMSE	MAE	d_{IA}	PBIAS	NSE	RSR	Grade
2016	P–T_a	0.9	0.81	0.7	0.54	0.95	−1.58	0.8	0.45	Excellent
	P–T_b	0.89	0.75	0.82	0.63	0.93	−3.14	0.74	0.52	Good
	P–T_c	0.59	0.62	0.97	0.8	0.86	−0.62	0.31	0.62	Unacceptable
2017	P–T_a	0.92	0.74	0.88	0.71	0.92	3.41	0.73	0.56	Good
	P–T_b	0.9	0.79	0.76	0.59	0.94	3.81	0.77	0.48	Good
	P–T_c	0.61	0.74	0.88	0.73	0.89	8.55	0.41	0.55	Unacceptable
2018	P–T_a	1.04	0.76	0.77	0.63	0.92	4.05	0.76	0.58	Good
	P–T_b	1.03	0.74	0.83	0.68	0.91	2.41	0.73	0.63	Adequate
	P–T_c	0.69	0.66	0.79	0.66	0.89	5.38	0.51	0.59	Adequate
2019	P–T_a	0.96	0.82	0.71	0.57	0.95	3.19	0.82	0.45	Excellent
	P–T_b	0.92	0.83	0.67	0.55	0.95	3.5	0.82	0.43	Excellent
	P–T_c	0.59	0.72	0.9	0.73	0.88	7.73	0.35	0.57	Unacceptable

The R^2 values for P–T_a and P–T_b during the four years ranged from 0.74 to 0.81, and the linear regression slopes ("b") ranged from 0.89 to 1.04, indicating that the model deviation is low. RMSE and MAE values were 0.67–0.88 and 0.54–0.71, respectively, indicating that the errors were within the allowable range. Both models exhibited good simulation of jujube evapotranspiration. However, as graded by RSR and NSE, P–T_a simulation accuracy was slightly higher than that for P–T_b. The model grades from the RSR and NSE results were "Excellent" or "Good". Therefore, we determined that we would use P–T_a (Figure 7) to simulate jujube evapotranspiration.

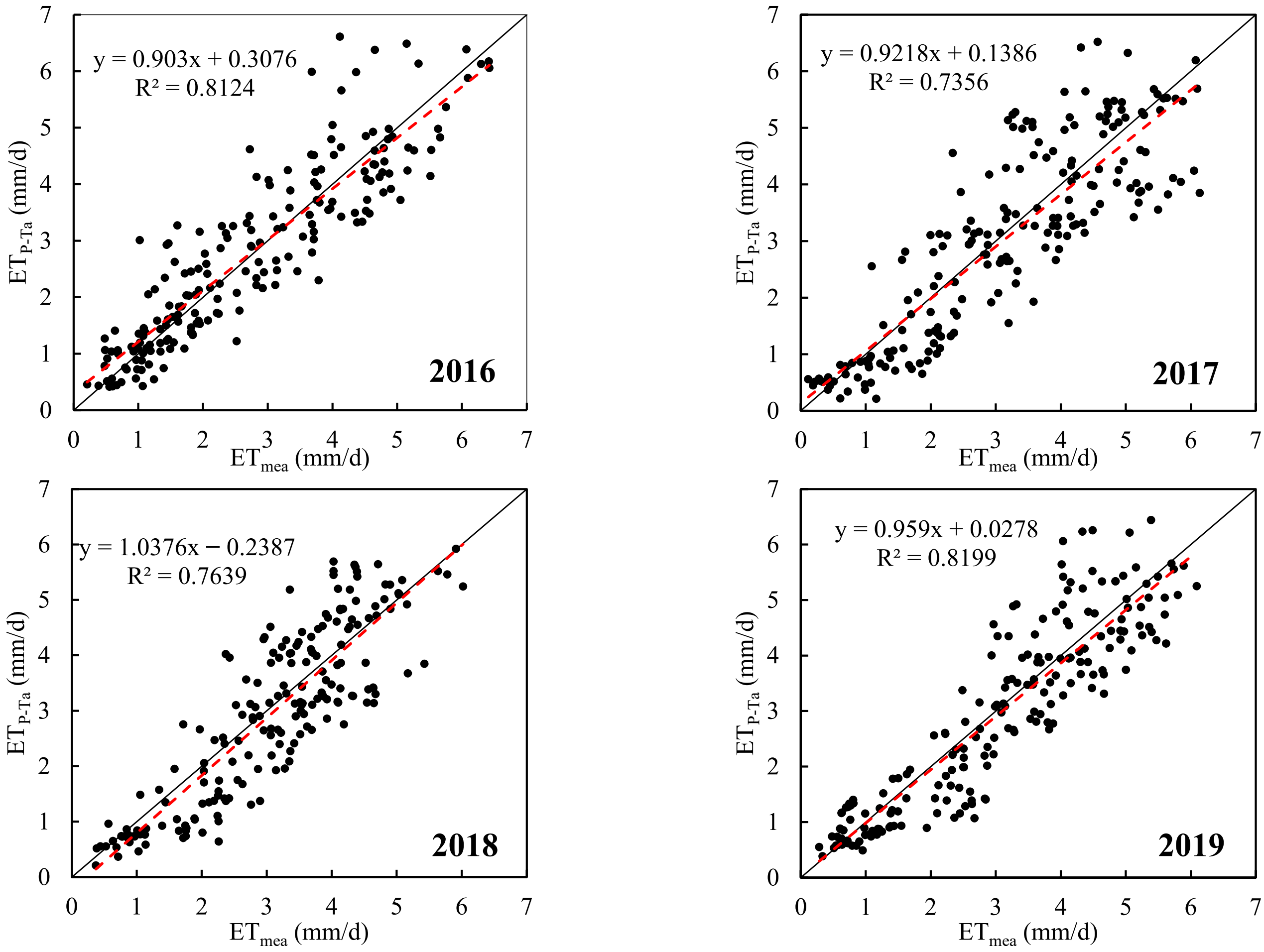

Figure 7. Comparisons of daily jujube evapotranspiration (ET) estimated with the P–Ta model and measured using a large weighing lysimeter during the 2016–2019 study period in the Aksu region, Xinjiang, China.

3.3. Comparisons of Daily Jujube ET Estimated with the Dual Kc Model and Measured Using a Large Weighing Lysimeter

Comparisons between daily ET estimated with the Dual Kc model ($ET_{Dual\ Kc}$) and measured using a large weighing lysimeter (ET_{mea}) from 2016–2019 are presented in Figure 8 and Table 9. Variations in daily $ET_{Dual\ Kc}$ were generally similar to those observed for ET_{mea}. The coefficients of determination (R^2) ranged from 0.82 to 0.87, and linear regression slopes (b) ranged from 0.92 to 1.00, indicating that the simulated and measured values were statistically similar. RMSE and MAE values were 0.60–0.82 and 0.46–0.66, respectively, indicating that errors were within the allowable range (Table 5). The d_{IA} ranged from 0.94 to 0.96, indicating that the residual variance was small and within the tolerance allowed for simulation error. PBIAS was greater than 0, indicating that the Dual Kc model generally underestimated ET. The simulation results for Dual Kc during the four years were graded by NSE and RSR values as "Excellent". Therefore, the simulation of jujube ET with the Dual Kc model was excellent, and the model produced little error.

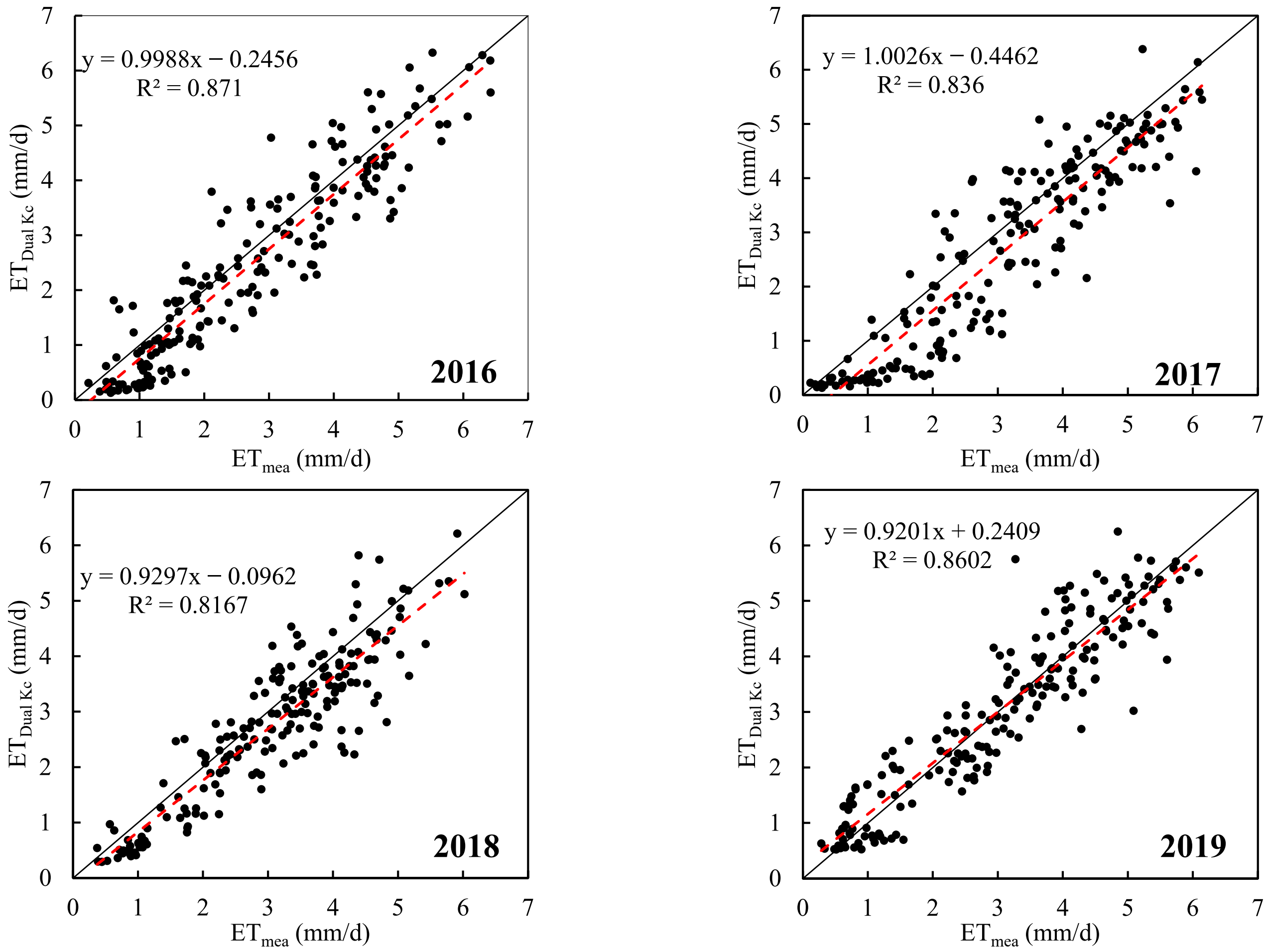

Figure 8. Comparisons of daily jujube evapotranspiration (ET) estimated with the Dual Kc model and measured using a large weighing lysimeter during the 2016–2019 study period in the Aksu region, Xinjiang, China.

Table 9. Error analysis for daily jujube evapotranspiration (ET) estimated with the Dual-Kc, S–W, and P–T models compared with ET measured using a large weighing lysimeter during the 2016–2019 study period in the Aksu region, Xinjiang, China.

Year	Model	b	R^2	RMSE (mm/d)	MAE (mm/d)	d_{IA}	PBIAS	NSE	RSR	Grade
2016	Dual Kc	1.00	0.87	0.65	0.53	0.96	8.93	0.85	0.41	Excellent
	S–W	0.83	0.79	0.74	0.61	0.94	−2.90	0.75	0.47	Excellent
	P–T_a	0.90	0.81	0.70	0.54	0.95	−1.58	0.80	0.45	Excellent
2017	Dual Kc	1.00	0.84	0.82	0.66	0.94	13.78	0.79	0.50	Excellent
	S–W	0.84	0.81	0.81	0.66	0.93	13.50	0.72	0.50	Good
	P–T_a	0.92	0.74	0.88	0.71	0.92	3.41	0.73	0.56	Good
2018	Dual Kc	0.93	0.82	0.66	0.53	0.94	10.18	0.77	0.49	Excellent
	S–W	0.89	0.74	0.93	0.79	0.88	20.24	0.61	0.64	Adequate
	P–T_a	1.04	0.76	0.77	0.63	0.92	4.05	0.76	0.58	Good
2019	Dual Kc	0.92	0.86	0.60	0.46	0.96	0.06	0.85	0.38	Excellent
	S–W	0.80	0.82	0.94	0.76	0.90	22.05	0.63	0.55	Adequate
	P–T_a	0.96	0.82	0.71	0.57	0.95	3.19	0.82	0.45	Excellent

Note: b, regression slope; R^2, coefficient of determination; RMSE, root mean square error; MAE, mean absolute error; NSE, Nash–Sutcliffe efficiency; RSR, ratio of RMSE to the standard deviation of observed data; d_{IA}, index of agreement; PBIAS, percent bias.

3.4. Comparisons of Daily Jujube ET Estimated with the S–W Model and Measured Using a Large Weighing Lysimeter

Comparisons between daily ET estimated with the S–W model ($ET_{S–W}$) and measured using a large weighing lysimeter (ET_{mea}) from 2016–2019 are presented in Figure 9 and Table 9. Variations in daily $ET_{S–W}$ were generally similar to those observed for ET_{mea}. The R^2 and regression slope values for $ET_{S–W}$ vs. ET_{mea} during the four years ranged from 0.74 to 0.82 and from 0.80 to 0.89, respectively, indicating that the simulated and measured values were statistically similar, and that most of the variation in ET was explained by the model. RMSE and MAE values were 0.74–0.94 and 0.61–0.79, respectively, indicating that model error was within the allowable range. The simulation results of S–W during 2016, 2017, 2018, and 2019 were graded by NSE and RSR as "Excellent", "Good", "Adequate", and "Adequate", respectively. The d_{IA} ranged from 0.88 to 0.94, indicating that the residual variance was relatively small and within the tolerance of allowable simulation error. Excluding 2016, PBIAS ranged from 13.50 to 18.05. The deviation of model simulation results was small, and the model noticeably and fairly consistently underestimated ET. Therefore, the S–W model may produce large errors.

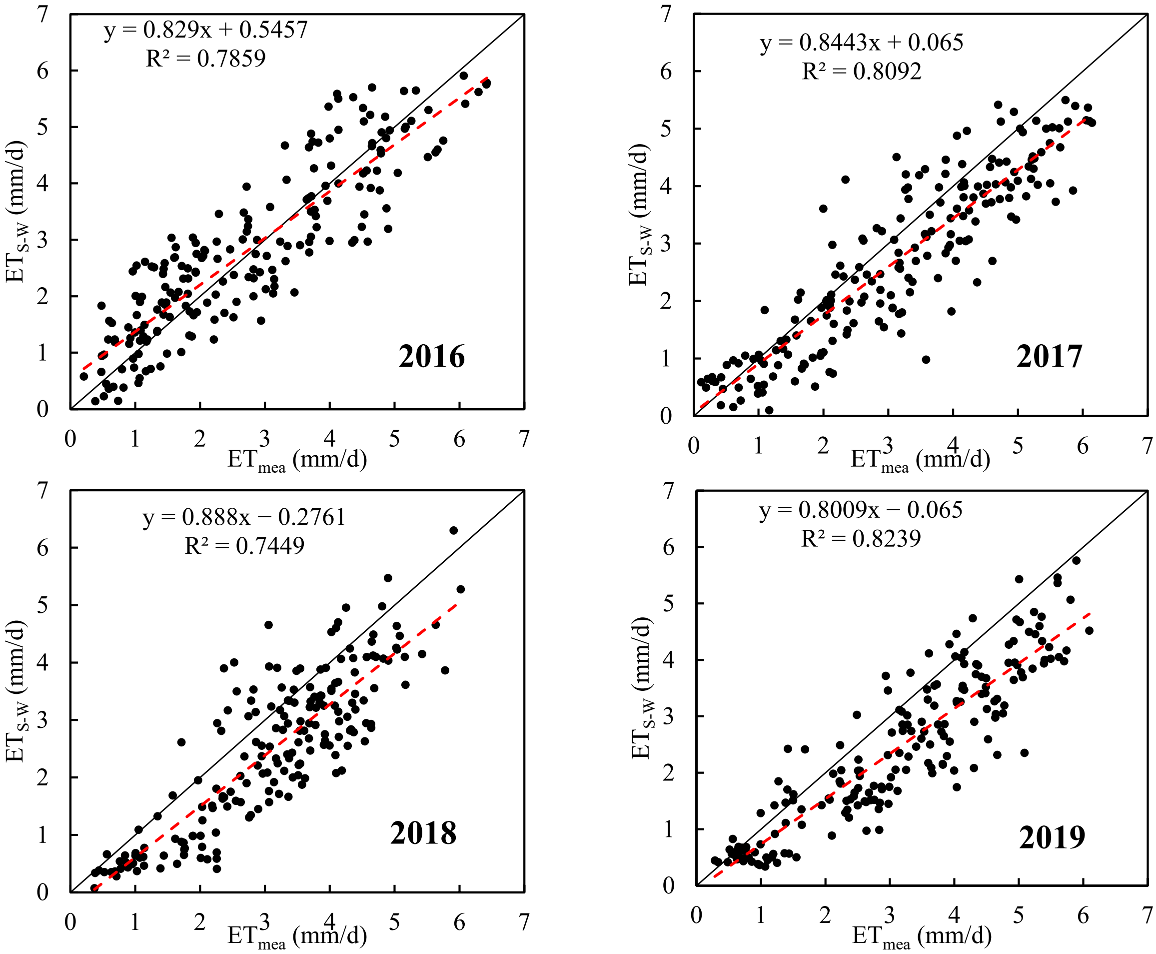

Figure 9. Comparisons of daily jujube evapotranspiration (ET) estimated with the S–W model and measured using a large weighing lysimeter during 2016–2019 in the Aksu region, Xinjiang, China.

3.5. Comparisons of Measured Jujube ET and ET Simulated with Three Models

Comparisons of measured ET and ET simulated with the three models are presented in Figure 10 and Table 9. Based on the b, R^2, RMSE, and MAE values shown in Table 9, the simulation errors of the three ET models followed the order of P–T_a (small), Dual Kc (small), and S–W (large). Most of the variation in measured jujube ET could be explained by the P–T_a and Dual Kc model, and the estimation error was very small. The model evaluation statistics were b = 0.92–1.04, R^2 = 0.74–0.87, RMSE = 0.60–0.88 mm/d, and MAE = 0.46–0.71 mm/d. The values of d_{IA} showed that the residual errors of the three models followed the order of Dual Kc < P–T_a < S–W model. The NSE and RSR values for the three models indicated that simulation ability for the three models followed the order of Dual Kc > P–T_a > S–W model. The stability of the Dual Kc model was significantly higher than that of the other two models during the four-year period. However, it can be seen from PBIAS that the deviation degree of the Dual Kc model consistently underestimated ET (PBIAS = 0.06–10.78%), and by a higher amount than the P–T_a model (PBIAS = −1.58–4.05%). In summary, the deviation degree of the P–T_a model was the lowest of the three models. The fitting results for the S–W model were "Good", but the deviation degree of the model was higher. The deviation degree of the Dual Kc model, however, was higher than that of the P–T_a model, and the fitting effect of the model was "Excellent" during the four-year period. The simulation effect of the model was stable. Thus, we suggest that the Dual Kc model be used as the preferred model to estimate jujube ET in order to improve irrigation scheduling for jujube grown in this arid area.

The absolute simulation errors at different growth stages were also compared for the three models. As can be seen from Figure 11, the absolute errors for the S–W model and the Dual Kc model were similar at budding, and were less than with the P–T_a model. The simulation error for the Dual Kc model was relatively less than that of the S–W model and the P–T_a model in the flowering, fruit setting, and fruit enlargement stages. At fruit maturity, the absolute error by the three models was similar, and underestimated jujube ET. In general, the absolute error produced by the Dual Kc model was the smallest over the entire growth period, followed by the S–W and P–T_a model.

3.6. Model Sensitivity Analysis

The results of the sensitivity analysis for six basic parameters (air temperature: T_a; relative humidity: RH; solar radiation: R_n; leaf area index: LAI; plant height: h_c; soil moisture content: θ) in the three models and six core parameters (VPD, r_a^c, r_s^c, r_a^a, r_s^s, r_a^s) in the S–W model are shown in Figure 12 and Table 10. ET, as simulated with the P–T_a model, was primarily affected by net radiation and air temperature. The model was "very sensitive" to net radiation and "sensitive" to temperature. Plant height, soil moisture, and net radiation had the greatest impact on the S–W simulation results, and they are "relatively sensitive" parameters in the model. Wind speed and relative humidity had little influence on ET simulated with the S–W model, and hence were classified as only "minor sensitivity". A special result from the sensitivity analysis was obtained for the Dual Kc model, and simulated ET was not sensitive to the model parameters.

In addition, it can be seen from Table 10 that r_a^a and r_s^c had the greatest impact on simulated jujube ET. When they changed by ±20%, ET changed by −5.62–5.12%. ET changed in response to ±20% changes in VPD and r_s^s with a range of −2.05–1.86%. r_a^c and r_a^s had the least effect, with ET only changing by −0.62–0.60%. In general, canopy resistance and the relationship between jujube canopy height and reference height had the greatest impact on ET. Other aerodynamic parameters had the least influence.

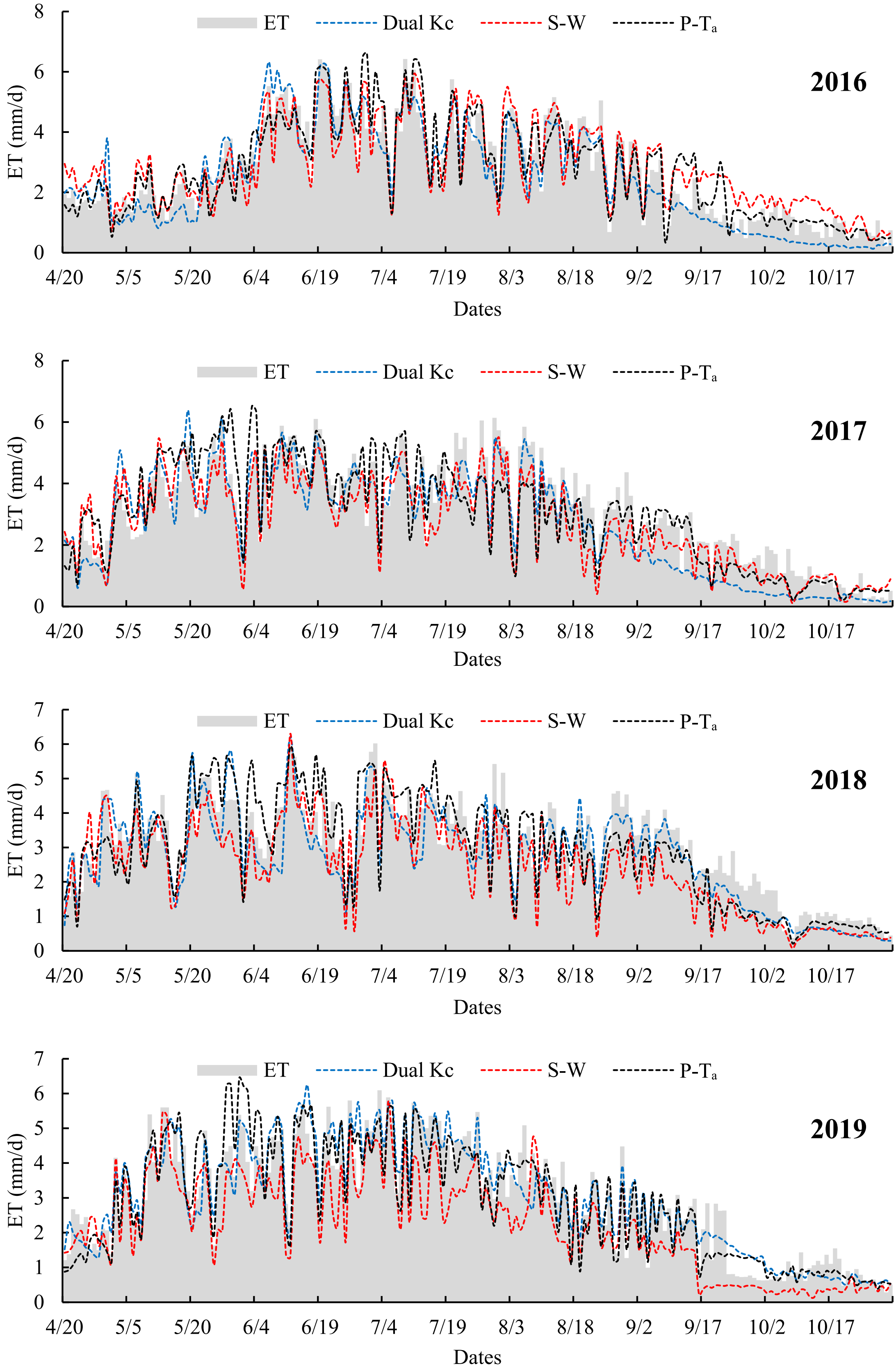

Figure 10. Time series of daily jujube evapotranspiration (ET) measured with a large weighing lysimeter, and ET values simulated with the Dual-Kc, S–W, and P–Ta models during the 2016–2019 study period in the Aksu region, Xinjiang, China.

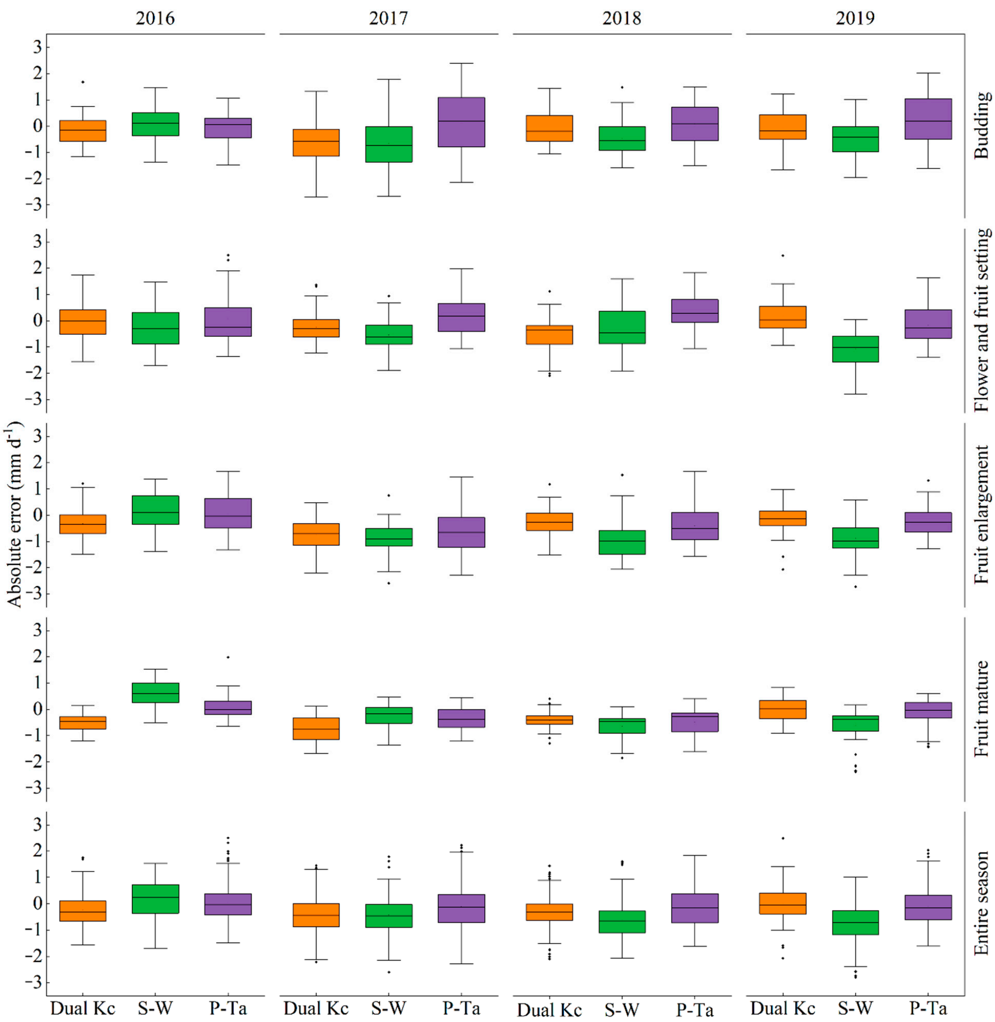

Figure 11. Boxplots of absolute errors for estimating daily jujube evapotranspiration with the Dual Kc, S–W, and P–Ta models at five growth stages during the 2016–2019 study period in the Aksu region, Xinjiang, China. Lower and upper box boundaries represent the 25th and 75th percentiles, respectively. The line and dot in the box represent the median and mean, respectively. The lower and upper whiskers represent the 5th and 95th percentiles, respectively. The dots beyond the whiskers represent outliers.

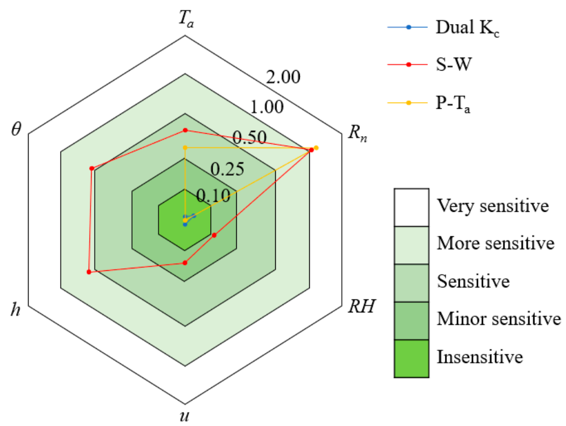

Figure 12. Relative sensitivity of simulated jujube evapotranspiration to the main input parameters for the P–Ta, S–W, and Dual-Kc models. T_a, air temperature; R_n, net radiation; RH, relative humidity; u, wind speed; h, plant height; θ, soil moisture.

Table 10. Sensitivity of simulated jujube evapotranspiration (ET) to ±20% changes in parameter values.

Model	Change in Parameter	T_a	R_n	RH	u	h	θ
S–W	−20%	−10.47%	−20.04%	−2.48%	3.13%	10.26%	−12.06%
	20%	7.35%	20.04%	2.27%	−2.98%	−10.72%	8.80%
Dual Kc	−20%	−1.44%	−1.78%	0.11%	−0.13%	−0.02%	
	20%	0.20%	0.73%	0.01%	0.11%	0.02%	
P–T_a	−20%	−6.12%	−25.00%				
	20%	6.08%	25.00%				
Model	**Change in Parameter**	VPD	r_a^c	r_s^c	r_a^a	r_s^s	r_a^s
S–W	−20%	1.86%	−0.62%	5.12%	−5.62%	1.53%	−0.11%
	20%	−2.05%	0.60%	−3.95%	4.84%	−1.40%	0.11%

Note: S–W, Shuttleworth–Wallace model; Dual Kc, dual crop coefficient model; P–T, Priestley–Taylor model; T_a, air temperature; R_n, net radiation; RH, relative humidity; u, wind speed; h, plant height; θ, soil moisture; VPD, vapor pressure deficit; r_a^c, boundary layer resistance; r_s^c, canopy resistance; r_s^s, soil surface resistance; r_a^a, aerodynamic resistance between vegetation canopy height and reference height; r_a^s, aerodynamic resistance between the soil surface and vegetation canopy.

4. Discussion

The P–T model has been commonly used to calculate crop ET under normal irrigation conditions [15,39]. When estimating crop ET with the P–T model, determining the value of the empirical coefficient "α" is crucial for effective use of the model. Some previous studies have shown that the value of "α" is strongly dependent on soil moisture, and that "α" increases with increasing soil moisture [40,41]. Therefore, conditions where soil moisture is stable will result in greater stability of model simulation accuracy. The P–T model has better adaptability in humid areas than other ET models [42]. However, Xinjiang is located in an arid area, with very high evaporative demand and large amounts surface soil water evaporation, resulting in great changes in soil moisture. Therefore, when the model is used, it is easy to produce a large error in simulated ET (Table 8). Bottazzi et al. [43] and Akumaga and Alderman [10] also confirmed this conclusion. Meanwhile, ET rates were underestimated when the soil was wet and overestimated when the soil was dry [44].

A previous study [45] has shown that the opening degree of the canopy (i.e., canopy cover) has a significant impact on the empirical coefficient "α". Under conditions where the same crop was planted at different densities, a smaller opening degree of the canopy led to the downregulation of "α". The P–T model is an ET estimation model based on the assumption that the effect of atmospheric aerodynamics on ET is less than the effect of radiation [46]. When air in the plant canopy is saturated or nearly saturated with water vapor, "α" is greater than 1.0. However, when the canopy opening degree is large (sparse planting pattern) or an agro-pastoral ecotone ecosystem is present, energy transmission will be significantly driven by the atmosphere, resulting in an obvious downregulation of "α" [47]. For example, in our study, the air flow around jujube trees and at the bottom of the canopy was large, and the boundary effect was obvious, such that the mean value of "α" was 0.64 over the entire growth period. Liang et al. [48] showed that under a sparse planting pattern in an arid area, "α" = 0.23. This result also shows that one of the reasons for the low estimation accuracy of sparse vegetation ET simulations is that the influence of canopy aerodynamics leads to an instability in "α" during the entire crop growing season [49], resulting in a large simulation error. Therefore, after improving the calculation method of "α" by using either linear fitting for different growth periods or a quadratic function over the entire growth period, the R^2 of the model increased from 0.62–0.74 to 0.74–0.83 (Table 8).

The basal crop coefficient is a crucial parameter in accurately simulating crop ET in the Dual Kc model, and its accurate determination is affected by many factors. Therefore, the crop coefficient recommended in FAO-56 should be adaptively adjusted according to regional differences and crop types. Bellvert et al. [50] showed that the median crop coefficient was related to orchard age and density. For large trees, a highly developed canopy and high leaf area index are the main factors that will increase the basal crop coefficient [51]. Therefore, young trees and low-density planting in orchards may lead to a reduction in crop coefficient values [52]. In our study, after trial-and-error adjustments, the crop coefficients of young jujube trees grown in an arid area were reduced by 0.10–0.15. In addition, there have been some reports that high wind speed and low vapor pressure increase stomatal conductance and crop coefficient values [53]. In areas with frequent rainy seasons or heavy rainfall, the crop coefficient will remain high [54]. The REW (readily evaporable water) and Z_e (depth of topsoil dried by evaporation) are core parameters for calculating topsoil evaporation. Some existing studies have shown that ET simulated with the Dual Kc model is underestimated when crop ET is abnormally high [55]. In our study, when jujube ET was abnormally high, ET was overestimated before mid-June. After mid-June, jujube ET was underestimated (Figure 8). We believe that tree crown width will appreciably affect the amount of thermal radiation energy received by the soil surface [8], thus affecting the values of REW and Z_e, especially during high-temperature time periods [56]. Therefore, the REW and Z_e should be adjusted by a factor to account for canopy shading, leaf area index, and environmental factors. In addition, some other studies [57] have also proven that simulated soil evaporation estimation using the Dual Kc model is poor in the early stages of crop growth. When canopy density is high, simulation errors for soil evaporation decrease significantly. Under this condition, the error caused by using fixed values of REW and Z_e is less and can easily be ignored.

The S–W model further optimizes the Penman–Monteith model mainly through soil surface resistance, canopy surface resistance, and three aerodynamic resistances. After sensitivity analysis of parameters, r_s^c and r_a^a were found to have the greatest impact on ET. This result is similar to results reported by Mu et al. [58]. r_s^c is mainly affected by leaf area index and soil moisture. Lower leaf area index may lead to ET overestimation by the model [59]. In addition, some studies have reported that a model of the water vapor exchange process involving stomatal control of the leaf/air interface is easy to build under stable soil water supply conditions [18]. However, when affected by water stress, plant stress resistance will cause changes to the minimum leaf stomatal resistance and to other related parameters, resulting in the obvious underestimation of crop ET [60], as was also found in our study. Therefore, the S–W model does not consider the effect of water stress on canopy surface resistance.

We attempted to use the P–T model, the S–W model, and the Dual Kc model to simulate the ET of young jujube trees in an arid area, and to compare simulated ET with ET measured using a large weighing lysimeter. Previous studies have shown that the S–W, P–T, and Dual Kc models can estimate ET in different ecosystems well [2,7,18]. However, the three models all have different errors in simulating ET that can be attributed to the inaccurate estimation of the effective energy of the surface soil and canopy caused by a variety of factors [58]. Among them, the ET simulation error of the P–T model was significantly higher than that of the S–W model and the Dual Kc model, mainly caused by changes in canopy aerodynamic resistance that caused "α" to fluctuate over the entire growth period. Therefore, after improving the calculation method for "α" by using either linear fitting for different growth periods or a quadratic function over the entire growth period, the simulation accuracy of the P–T model was significantly improved. For the S–W model, the results showed that the S–W error was higher than for the Dual Kc model. Our analysis showed that the reasons for the large error in ET simulations by the S–W model were as follows: (1) assuming that soil moisture is basically constant, then the stomatal model in the S–W model is suitable; however, after irrigation or rainfall, the soil moisture content changes greatly, and the simulated stomatal resistance value is higher than the actual value, resulting in the simulated value of ET being lower than the measured value under the wetter conditions following irrigation or rainfall; (2) the S–W model does not consider differences in albedo and emitted longwave radiation between the soil surface and the canopy, leading to an increase in model simulation error; (3) in areas where water-saving irrigation technologies such as furrow irrigation, drip irrigation, and small pipe outflow are used, the spatial variability of surface moisture is very large, resulting in reduced simulation accuracy.

5. Conclusions

(1) After improving the calculation method of "α" by using either linear fitting for different growth periods (P–T_a) or a quadratic function over the entire growth period (P–T_b), the R^2 of the P–T model increased from 0.62–0.74 to 0.74–0.83. Both of the improved models provided good simulations of jujube evapotranspiration. Simulation accuracy was slightly higher for P–T_a than for P–T_b.

(2) The basal crop coefficients of the modified Dual Kc model at the initial, middle, and end stages of development were 0.4, 1.0, and 0.5, respectively. The error analysis results showed that the overall simulation error for the Dual Kc model was low, and that the model simulation was stable. However, simulation accuracy decreased when there was severe water deficit, resulting in jujube ET being significantly underestimated.

(3) Simulation error for the S–W model was larger than for the other models, and the model generally underestimated ET. In addition, it can be seen from the NSE and RSR values that S–W simulations were the worst and most unstable of the three models.

(4) Through our comprehensive evaluation of these three ET models we conclude that the simulation abilities of the Dual Kc model and P–T_a model were similar, and slightly better than the S–W model. The simulation effect grade for the Dual Kc model was "Excellent" during the four years of the study, and the simulation stability was higher than that observed for the P–T_a model. The P–T_a model was easily affected by changes in net radiation and air temperature due to the few formula parameters. Therefore, the Dual Kc model had better performance than the S–W model and the P–T_a model in estimating jujube ET and could be recommended to estimate jujube ET.

Author Contributions: Conceptualization, P.A. and Y.M.; methodology, P.A.; writing—review and editing, P.A., Y.M. and Y.H. All authors have read and agreed to the published version of the manuscript.

Funding: This work was supported by The Central Guidance on Local Science and Technology Development Fund (ZYYD2023A10), the National Natural Science Foundation of China (52069027), and the Fund of Academician Mingjiang Deng Workstation (2020.D-003).

Conflicts of Interest: The authors declare no conflict of interest.

References

1. SBX. *Xinjiang Statistical Yearbook in 2019*; China Statistical Publishing House: Ürümqi, China, 2020.
2. Anupoju, V.; Kambhammettu, B.V.N.P. Role of deficit irrigation strategies on ET partition and crop water productivity of rice in semi-arid tropics of south India. *Irrig. Sci.* **2020**, *38*, 415–430. [CrossRef]
3. Raphael, O.; Ogedengbe, K.; Fasinmirin, J.; Okunade, D.; Akande, I.; Gbadamosi, A. Growth-stage-specific crop coefficient and consumptive use of Capsicum chinense using hydraulic weighing lysimeter. *Agric. Water Manag.* **2018**, *203*, 179–185. [CrossRef]
4. García-Tejero, I.; López-Borrallo, D.; Miranda, L.; Medina, J.; Arriaga, J.; Muriel-Fernández, J.; Martínez-Ferri, E. Estimating strawberry crop coefficients under plastic tunnels in Southern Spain by using drainage lysimeters. *Sci. Hortic.* **2018**, *231*, 233–240. [CrossRef]
5. Allen, R.G.; Pereira, L.S.; Raes, D.; Smith, M. Crop Evapotranspiration: Guidelines for Computing Crop Water Requirements. In *FAO Irrigation and Drainage Paper 56*; FAO: Rome, Italy, 1998.
6. Tian, F.; Yang, P.; Hu, H.; Dai, C. Partitioning of Cotton Field Evapotranspiration under Mulched Drip Irrigation Based on a Dual Crop Coefficient Model. *Water* **2016**, *8*, 72. [CrossRef]
7. Peddinti, S.R.; Kambhammettu, B.P. Dynamics of crop coefficients for citrus orchards of central India using water balance and eddy covariance flux partition techniques. *Agric. Water Manag.* **2019**, *212*, 68–77. [CrossRef]
8. Rallo, G.; Paço, T.; Paredes, P.; Puig-Sirera, À.; Massai, R.; Provenzano, G.; Pereira, L. Updated single and dual crop coefficients for tree and vine fruit crops. *Agric. Water Manag.* **2021**, *250*, 106645. [CrossRef]
9. Lozano, D.; Ruiz, N.; Gavilán, P. Consumptive water use and irrigation performance of strawberries. *Agric. Water Manag.* **2016**, *169*, 44–51. [CrossRef]
10. Priestley, C.H.B.; Taylor, R.J. On the Assessment of Surface Heat Flux and Evaporation Using Large-Scale Parameters. *Mon. Weather Rev.* **1972**, *100*, 81–92. [CrossRef]

11. Akumaga, U.; Alderman, P.D. Comparison of Penman—Monteith and Priestley—Taylor Evapotranspiration Methods for Crop Modeling in Oklahoma. *Agron. J.* **2019**, *111*, 1171–1180. [CrossRef]
12. Ngongondo, C.; Xu, C.-Y.; Tallaksen, L.M.; Alemaw, B. Evaluation of the FAO Penman—Montheith, Priestley—Taylor and Hargreaves models for estimating reference evapotranspiration in southern Malawi. *Hydrol. Res.* **2013**, *44*, 706–722. [CrossRef]
13. Wang, X.; Zhang, B.; Li, F.; Li, X.; Li, X.; Wang, Y.; Shao, R.; Tian, J.; He, C. Vegetation restoration projects intensify intraregional water recycling processes in the agro-pastoral ecotone of Northern China. *J. Hydrometeorol.* **2021**, *22*, 1385–1403. [CrossRef]
14. Jobson, H.E. Evaporation Into the Atmosphere: Theory, History, and Applications. *Eos Trans. Am. Geophys. Union* **1982**, *63*, 1223. [CrossRef]
15. Flint, A.L.; Childs, S.W. Use of the Priestley-Taylor evaporation equation for soil water limited conditions in a small forest clearcut. *Agric. For. Meteorol.* **1991**, *56*, 247–260. [CrossRef]
16. Baldocchi, D. A comparative study of mass and energy exchange over a closed C3 (wheat) and an open C4 (corn) canopy: I. The partitioning of available energy into latent and sensible heat exchange. *Agric. For. Meteorol.* **1994**, *67*, 191–220. [CrossRef]
17. Shuttleworth, W.J.; Wallace, J.S. Evaporation from sparse crops-an energy combination theory. *Q. J. R. Meteorol. Soc.* **1985**, *111*, 839–855. [CrossRef]
18. Liu, X.; Xu, J.; Wang, W.; Lv, Y.; Li, Y. Modeling rice evapotranspiration under water-saving irrigation condition: Improved canopy-resistance-based. *J. Hydrol.* **2020**, *590*, 125435. [CrossRef]
19. Huang, S.; Yan, H.; Zhang, C.; Wang, G.; Acquah, S.J.; Yu, J.; Li, L.; Ma, J.; Darko, R.O. Modeling evapotranspiration for cucumber plants based on the Shuttleworth-Wallace model in a Venlo-type greenhouse. *Agric. Water Manag.* **2020**, *228*, 105861. [CrossRef]
20. Ortega-Farias, S.; Poblete-Echeverría, C.; Brisson, N. Parameterization of a two-layer model for estimating vineyard evapotranspiration using meteorological measurements. *Agric. For. Meteorol.* **2010**, *150*, 276–286. [CrossRef]
21. Meng, W.; Sun, X.; Ma, J.; Guo, X.; Lei, T.; Li, R. Measurement and simulation of the water storage pit irrigation trees evapotranspiration in the Loess Plateau. *Agric. Water Manag.* **2019**, *226*, 105804. [CrossRef]
22. Dong, J.; Yue, N.; Dang, H.; Wang, G.; Wei, G. Estimation of evapotranspiration in maize fields with ground mulching with plastic film in semi-arid areas using revised Shuttleworth-Wallace model. *Chin. J. Eco-Agric.* **2016**, *24*, 674–683. [CrossRef]
23. Ai, P.; Ma, Y.; Hai, Y. Jujube is at a competitiveness disadvantage to cotton in intercropped system. *Agron. J.* **2021**. [CrossRef]
24. Hong, M.; Zhu, H.; Mu, H.; Zhao, J.; Ma, Y. The water consumption rule of jujube trees under different emitter flow rate and irrigation quota. *Agric. Res. Arid Reg.* **2014**, *1*, 72–77.
25. Feigenwinter, C.; Franceschi, J.; Larsen, J.A.; Spirig, R.; Vogt, R. On the performance of microlysimeters to measure non-rainfall water input in a hyper-arid environment with focus on fog contribution. *J. Arid Environ.* **2020**, *182*, 104260. [CrossRef]
26. Zhou, M.C.; Ishidaira, H.; Hapuarachchi, H.P.; Magome, J.; Kiem, A.S.; Takeuchi, K. Estimating potential evapotranspiration using Shuttleworth–Wallace model and NOAA-AVHRR NDVI data to feed a distributed hydrological model over the Mekong River basin. *J. Hydrol.* **2006**, *327*, 151–173. [CrossRef]
27. Chen, F.; Dudhia, J. Coupling an advanced land surface-hydrology model with the Penn State-NCAR MM5 modeling system. Part I: Model implementation and sensitivity. *Mon. Weather Rev.* **2001**, *129*, 569–585. [CrossRef]
28. Gardiol, J.M.; Serio, L.A.; Della Maggiora, A.I. Modelling evapotranspiration of corn (Zea mays) under different plant densities. *J. Hydrol.* **2003**, *271*, 188–196. [CrossRef]
29. Tourula, T.; Heikinheimo, M. Modelling evapotranspiration from a barley field over the growing season. *Agric. For. Meteorol.* **1998**, *91*, 237–250. [CrossRef]
30. Villagarcía, L.; Were, A.; García, M.; Domingo, F. Sensitivity of a clumped model of evapotranspiration to surface resistance parameterisations: Application in a semi-arid environment. *Agric. For. Meteorol.* **2010**, *150*, 1065–1078. [CrossRef]
31. Crow, W.T.; Kustas, W.P.; Prueger, J.H. Monitoring root-zone soil moisture through the assimilation of a thermal remote sensing-based soil moisture proxy into a water balance model. *Remote Sens. Environ.* **2008**, *112*, 1268–1281. [CrossRef]
32. Noilhan, J.; Planton, S. A Simple Parameterization of Land Surface Processes for Meteorological Models. *Mon. Weather Rev.* **1989**, *117*, 536–549. [CrossRef]
33. Kato, T.; Kimura, R.; Kamichika, M. Estimation of evapotranspiration, transpiration ratio and water-use efficiency from a sparse canopy using a compartment model. *Agric. Water Manag.* **2004**, *65*, 173–191. [CrossRef]
34. Yang, L.; Gao, Y.; Han, M.; Shen, X.; Gong, W.; Duan, A. Simulation of Soil Moisture Dynamics and Soil Evaporation of Winter Wheat Based on SIMDual_Kc Model in Northern Henan Province. *J. Soil Water Conserv.* **2016**, *30*, 147–153. [CrossRef]
35. Gonzalez-Ollauri, A.; Stokes, A.; Mickovski, S.B. A novel framework to study the effect of tree architectural traits on stemflow yield and its consequences for soil-water dynamics. *J. Hydrol.* **2020**, *582*, 124448. [CrossRef]
36. Choi, J.Y.; Choi, C.-H. Sensitivity analysis of multilayer perceptron with differentiable activation functions. *IEEE Trans. Neural Netw.* **1992**, *3*, 101–107. [CrossRef] [PubMed]
37. Rosa, R.D.; Paredes, P.; Rodrigues, G.C.; Fernando, R.M.; Alves, I.; Pereira, L.S.; Allen, R.G. Implementing the dual crop coefficient approach in interactive software: 2. Model testing. *Agric. Water Manag.* **2012**, *103*, 62–77. [CrossRef]
38. Wang, Z.; Cai, H.; Yu, L.; Wang, X.; Shi, X. Estimation of evapotranspiration and soil evaporation of winter wheat in arid region of Northwest China based on SIMDualKc model. *Trans. Chin. Soc. Agric. Eng.* **2016**, *32*, 126–136. [CrossRef]
39. Song, L.; Kustas, W.P.; Liu, S.; Colaizzi, P.D.; Nieto, H.; Xu, Z.; Ma, Y.; Li, M.; Xu, T.; Agam, N.; et al. Applications of a thermal-based two-source energy balance model using Priestley-Taylor approach for surface temperature partitioning under advective conditions. *J. Hydrol.* **2016**, *540*, 574–587. [CrossRef]

40. Gong, X.; Qiu, R.; Ge, J.; Bo, G.; Ping, Y.; Xin, Q.; Wang, S. Evapotranspiration partitioning of greenhouse grown tomato using a modified Priestley—Taylor model. *Agric. Water Manag.* **2021**, *247*, 106709. [CrossRef]
41. Qiu, R.; Liu, C.; Cui, N.; Wu, Y.; Wang, Z.; Li, G. Evapotranspiration estimation using a modified Priestley-Taylor model in a rice-wheat rotation system. *Agric. Water Manag.* **2019**, *224*, 105755. [CrossRef]
42. Wu, H. Evapotranspiration estimation of Platycladus orientalis in Northern China based on various models. *J. For. Res.* **2016**, *27*, 871–878. [CrossRef]
43. Bottazzi, M.; Bancheri, M.; Mobilia, M.; Bertoldi, G.; Longobardi, A.; Rigon, R. Comparing Evapotranspiration Estimates from the GEOframe-Prospero Model with Penman–Monteith and Priestley-Taylor Approaches under Different Climate Conditions. *Water* **2021**, *13*, 1221. [CrossRef]
44. Guo, J.; Li, Q.; Yan, C.; Mei, X.; Li, Y. Effects of small area irrigation on water and heat transport of winter wheat field under drought condition. *Trans. Chin. Soc. Agric. Eng.* **2008**, *24*, 20–24. [CrossRef]
45. Ramarohetra, J.; Sultan, B. Impact of ET0 method on the simulation of historical and future crop yields: A case study of millet growth in Senegal. *Int. J. Climatol.* **2018**, *38*, 729–741. [CrossRef]
46. Gan, G.; Liu, Y. Inferring transpiration from evapotranspiration: A transpiration indicator using the Priestley-Taylor coefficient of wet environment. *Ecol. Indic.* **2020**, *110*, 105853. [CrossRef]
47. Tong, X.; Zhang, J.; Meng, P.; Li, J.; Zheng, N. Environmental controls of evapotranspiration in a mixed plantation in North China. *Int. J. Biometeorol.* **2017**, *61*, 227–238. [CrossRef]
48. Liang, C.; Ma, J.; Yang, R.; Tian, Y.; Jiao, X.; Cha, T.; Yang, L. Priestley-Taylor model coefficient in a typical Artemisia ordosica shrubland in Mu Us Sandy Land of northwestern China. *J. Beijing For. Univ.* **2018**, *40*, 1–8. [CrossRef]
49. Tongwane, M.I.; Savage, M.J.; Tsubo, M.; Moeletsi, M.E. Seasonal variation of reference evapotranspiration and Priestley-Taylor coefficient in the eastern Free State, South Africa. *Agric. Water Manag.* **2017**, *187*, 122–130. [CrossRef]
50. Bellvert, J.; Adeline, K.; Baram, S.; Pierce, L.; Sanden, B.L.; Smart, D.R. Monitoring Crop Evapotranspiration and Crop Coefficients over an Almond and Pistachio Orchard Throughout Remote Sensing. *Remote Sens.* **2018**, *10*, 2001. [CrossRef]
51. Cammalleri, C.; Ciraolo, G.; Minacapilli, M.; Rallo, G. Evapotranspiration from an Olive Orchard using Remote Sensing-Based Dual Crop Coefficient Approach. *Water Resour. Manag.* **2013**, *27*, 4877–4895. [CrossRef]
52. Espadafor, M.; Orgaz, F.; Testi, L.; Lorite, I.J.; Villalobos, F.J. Transpiration of young almond trees in relation to intercepted radiation. *Irrig. Sci.* **2015**, *33*, 265–275. [CrossRef]
53. Rana, G.; Katerji, N.; de Lorenzi, F. Measurement and modelling of evapotranspiration of irrigated citrus orchard under Mediterranean conditions. *Agric. For. Meteorol.* **2005**, *128*, 199–209. [CrossRef]
54. Er-Raki, S.; Chehbouni, A.; Guemouria, N.; Ezzahar, J.; Khabba, S.; Boulet, G.; Hanich, L. Citrus orchard evapotranspiration: Comparison between eddy covariance measurements and the FAO-56 approach estimates. *Plant Biosyst. Int. J. Deal. All Asp. Plant Biol.* **2009**, *143*, 201–208. [CrossRef]
55. Ai, P.; Ma, Y. Estimation of Evapotranspiration of a Jujube/Cotton Intercropping System in an Arid Area Based on the Dual Crop Coefficient Method. *Agriculture* **2020**, *10*, 65. [CrossRef]
56. Darouich, H.; Karfoul, R.; Ramos, T.B.; Moustafa, A.; Shaheen, B.; Pereira, L.S. Crop water requirements and crop coefficients for jute mallow (*Corchorus olitorius* L.) using the SIMDualKc model and assessing irrigation strategies for the Syrian Akkar region. *Agric. Water Manag.* **2021**, *255*, 107038. [CrossRef]
57. Wu, N.; Yang, C.; Luo, Y.; Sun, L. Estimating Evapotranspiration and ItsComponents in Cotton Fields under DeficitIrrigation Conditions. *Pol. J. Environ. Stud.* **2019**, *28*, 393–405. [CrossRef]
58. Mu, Y.; Li, J.; Tong, X.; Zhang, J.; Meng, P.; Ren, B. Evapotranspiration simulated by Penman-Monteith and Shuttleworth-Wallace models over a mixed plantation in the southern foot of the Taihang Mountain, northern China. *J. Beijing For. Univ.* **2017**, *39*, 35–44. [CrossRef]
59. Wei, X.; Liu, S.; Chen, D.; Wang, Y.; Wang, X.; Wei, X. Applicability of Shuttleworth-Wallace Model for Evapotranspiration Estimation of Jujube Forests in Loess Hilly-gully Region. *Trans. Chin. Soc. Agric. Mach.* **2015**, *46*, 142–151. [CrossRef]
60. Gao, X.; Gu, F.; Gong, D.; Hao, W.; Chu, J.; Li, H. Comparison of three evapotranspiration models in a rain-fed spring maize filed in the Loess Plateau, China. *J. Agric. Meteorol.* **2020**, *76*, 155–163. [CrossRef]